Resistance to thyroid hormone is modulated in vivo by the nuclear receptor corepressor (NCOR1)

Laura Fozzatti[a], Changxue Lu[a], Dong Wook Kim[a], Jeong Won Park[a], Inna Astapova[b], Oksana Gavrilova[c], Mark C. Willingham[d], Anthony N. Hollenberg[b], and Sheue-yann Cheng[a,1]

[a]Laboratory of Molecular Biology, Center for Cancer Research, National Cancer Institute, National Institutes of Health, Bethesda, MD 20892; [b]Division of Endocrinology, Metabolism and Diabetes, Beth Israel Medical Center, Harvard Medical School, Boston, MA 02215; [c]National Institute of Diabetes, Digestive and Kidney Diseases, National Institutes of Health, Bethesda, MD 20892; and [d]Department of Pathology, Wake Forest University, Winston-Salem, NC 27157

Mutations in the ligand-binding domain of the thyroid hormone receptor β (TRβ) lead to resistance to thyroid hormone (RTH). These TRβ mutants function in a dominant-negative fashion to interfere with the transcription activity of wild-type thyroid hormone receptors (TRs), leading to dysregulation of the pituitary–thyroid axis and resistance in peripheral tissues. The molecular mechanism by which TRβ mutants cause RTH has been postulated to be an inability of the mutants to properly release the nuclear corepressors (NCORs), thereby inhibiting thyroid hormone (TH)-mediated transcription activity. To test this hypothesis in vivo, we crossed *Thrb^PV* mice (a model of RTH) expressing a human TRβ mutant (PV) with mice expressing a mutant *Ncor1* allele (*Ncor1^ΔID* mice) that cannot recruit a TR or a PV mutant. Remarkably, in the presence of NCOR1ΔID, the abnormally elevated thyroid-stimulating hormone and TH levels found in *Thrb^PV* mice were modestly but significantly corrected. Furthermore, thyroid hyperplasia, weight loss, and other hallmarks of RTH were also partially reverted in mice expressing NCOR1ΔID. Taken together, these data suggest that the aberrant recruitment of NCOR1 by RTH TRβ mutants leads to clinical RTH in humans. The present study suggests that therapies aimed at the TR–NCOR1 interaction or its downstream actions could be tested as potential targets in treating RTH.

thyroid hormone receptor mutant | mouse models | dominant negative activity

Thyroid hormone (TH) signaling plays a crucial role in developing and maintaining metabolic homeostasis in humans. The genomic actions of TH are mediated by the thyroid hormone receptor (TR) isoforms α1, β1, and β2, which regulate target genes in the presence or absence of TH via recruitment of coregulatory complexes (1, 2). In the absence of T3 on target genes that are positively regulated by T3, TRs recruit the nuclear corepressors NCOR1 and NCOR2 for transcriptional repression. The addition of T3 leads to a conformational change in the TR that releases the NCOR1/NCOR2 complex and allows for the recruitment of a multiprotein coactivator complex for transcriptional activation (3). Recent advances made by our group and others have expanded this model and shown that NCOR1 and NCOR2 play a role in determining T3 sensitivity in vivo, suggesting that corepressors can be recruited to TR in the presence of T3 (4–6).

Resistance to thyroid hormone (RTH) is an autosomal dominant human disease due to mutations in the thyroid hormone receptor β (TRβ) ligand-binding domain that prevent T3 binding and alter coregulator recruitment. RTH manifests itself by an inappropriately elevated thyroid-stimulating hormone (TSH) in the face of increased TH levels and with a complex clinical phenotype (7). Knock-in mouse models that faithfully recreate the human disease and provide an opportunity to explore novel therapeutic approaches to the disorder have been developed (8, 9).

Although RTH TRβ mutations are predicted to impair T3-mediated activation or repression of target genes, the exact mechanism of action of these dominant negative mutants has not been elucidated in vivo. Earlier work has established that TRβ mutants can compete directly with the wild-type TR for DNA

binding and also compete for limiting coregulators, thus impairing transcriptional activation by wild-type TRs (10, 11). However, subsequent cell culture experiments have demonstrated that constitutive recruitment of NCOR1/NCOR2 was critical to the dominant negative phenotype of TRβ mutants (12, 13). A similar hypothesis has been put forward for the peroxisome proliferator-activated receptor γ ligand-binding domain mutants that cause lipodystrophy (14). If this were the case, then abrogation of the TRβ mutant–NCOR1/NCOR2 interaction should ameliorate the syndrome of RTH, and this outcome would suggest a therapeutic strategy for the disorder.

To test this hypothesis, we took advantage of a mouse model of human RTH, the *Thrb^PV* mouse that harbors a knock-in mutation (denoted PV) of the *Thrb* gene (8). The PV mutation, identified in a patient with RTH, has a frame-shift mutation in the C-terminal 14 amino acids, resulting in the complete loss of T3-binding activity and transcription capacity (15). *Thrb^PV* mice reproduce human RTH with elevated TH levels accompanied by nonsuppressible serum TSH levels and other abnormalities similar to human RTH (7). We crossed *Thrb^PV* mice with mice that globally express an NCOR1 mutant protein (NCOR1ΔID) in which the receptor interaction domains have been modified so that it cannot interact with the TR (5). We have previously shown that *Ncor1^ΔID* mice have increased sensitivity to TH and a normal TSH despite low T4 and T3 levels, demonstrating the specificity of NCOR1 for regulating the thyroid axis in vivo (6). Remarkably, expression of NCOR1ΔID protein in heterozygous and homozygous *Thrb^PV* mice significantly normalized the dysregulation of the pituitary–thyroid axis and other abnormalities in peripheral target tissues. Thus, strategies directed against NCOR1 recruitment or the complex that it recruits could potentially serve as therapeutic targets for this disorder.

Results

PV Does Not Interact with NCOR1ΔID. We have shown previously that NCOR1ΔID lacking the N3 and N2 receptor-interacting domains prevents recruitment of TR in vivo (5). To confirm that NCOR1ΔID is also unable to recruit PV, we performed coimmunoprecipitation studies both in transfected 293T cells and in vivo in wild-type (WT), *Thrb^{PV/PV}Ncor1^{+/+}*, and *Thrb^{PV/PV} Ncor1^{ΔID/ΔID}* mice. In 293T cells expressing PV via viral transduction and transfected with expression plasmid of NCOR1, specific antiserum directed against PV (#302) interacted with NCOR1 (lane 3, Fig. 1A). In contrast, when PV-expressing cells were transfected with NCOR1ΔID, PV interacted only with the endogenous NCOR1 (lane 6, Fig. 1A), not with the faster-migrating NCOR1ΔID (lower band, lane 8, Fig. 1A). To confirm that this was the case in vivo, we carried out similar coimmu-
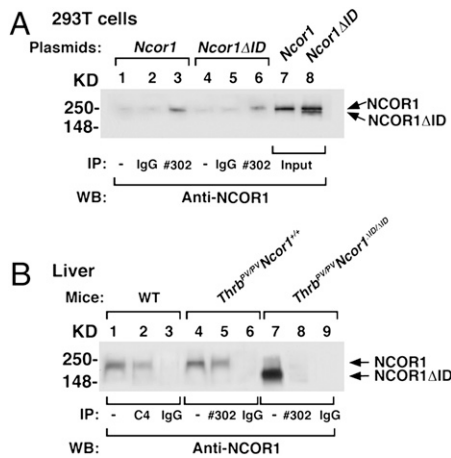
Fig. 1. PV cannot recruit NCOR1ΔID in vitro or in vivo. (*A*) 293T cells were transduced with a PV-expressing viral vector followed by transfection with a *Ncor1* expression plasmid (lanes 1–3) or a *Ncor1ΔID* expression plasmid (lanes 4–6). Total cellular extracts (1 mg) were immunoprecipitated with no antibody (lanes 1 and 4), IgG (lanes 2 and 5), or #302 antibody specifically against PV (lanes 3 and 6), followed by Western analysis using anti-NCOR1 antibody (2 μg/mL). A 2% input was used for direct Western blot analysis (lanes 7 and 8). (*B*) Nuclear extracts were prepared from the liver of WT mice (lanes 1–3), *Thrb^{PV/PV}Ncor1^{+/+}* mice (lanes 4–6), and *Thrb^{PV/PV}Ncor1^{ΔID/ΔID}* mice (lanes 7–9). Nuclear extracts (1.1 mg) were immunoprecipitated with mouse monoclonal anti-TR (C4), anti-PV (#302) antibodies, or IgG (control) followed by Western analysis using anti-NCOR1 antibody (2 μg/mL). Lanes 1, 4, and 7 represent input (~2%).

noprecipitation analysis from liver nuclear extracts (Fig. 1*B*). In the liver of WT mice, when anti-TR antibody (C4) was used in the immunoprecipitation followed by anti-NCOR1 antibodies, NCOR1 was clearly visible (lane 2, Fig. 1*B*). When anti-PV antibody was used to immunoprecipitate the liver nuclear extracts of *Thrb^{PV/PV}Ncor1^{+/+}* mice, PV interacted with NCOR1 (lane 5). In contrast, PV did not interact with NCOR1ΔID (lane 8) in the liver nuclear extracts of *Thrb^{PV/PV}Ncor1^{ΔID/ΔID}* mice. Thus, the cross of *Ncor1^{ΔID}* and *Thrb^{PV}* mice will allow us to determine if NCOR1 plays a role in the pathogenesis of RTH in vivo.

Deletion of Receptor Interaction Domains in NCOR1 Ameliorates RTH in the Pituitary–Thyroid Axis in Vivo. The hallmark of RTH is increased circulating levels of serum T3 and T4 accompanied by normal or elevated serum TSH levels (7). Indeed, the TRβPV

mutation in both mice and humans results in an elevated serum TSH in the presence of increased thyroid hormone levels (8). This phenotype is thought to be secondary to the ability of the mutant TRβ isoform to prevent negative regulation of TSH subunit genes in the pituitary by T3. To determine if the aberrant recruitment of NCOR1 by PV is responsible, we crossed *Thrb^{PV}* mice with *Ncor1^{ΔID}* mice and then assessed thyroid function in the resulting genotypes. Fig. 2*A* shows that, compared with WT mice (2.77 ± 0.21 μg/dL, n = 21), serum total T4 (TT4) decreased by 43% in *Thrb^{+/+}Ncor1^{ΔID/ΔID}* mice (1.58 ± 0.09 μg/dL, n = 11), a finding consistent with what we have shown previously and indicative of the importance of NCOR1 in establishing the set point of the thyroid axis (6). Remarkably, the elevated TT4 levels in *Thrb^{PV/+}Ncor1^{+/+}* mice (10.20 ± 0.51 μg/dL, n = 32) markedly decreased in *Thrb^{PV/+}Ncor1^{ΔID/ΔID}* mice (5.64 ± 0. 45 μg/dL, n = 17), representing a 45% reduction. Moreover, compared with the elevated TT4 of *Thrb^{PV/PV}Ncor1^{+/+}* mice (32.40 ± 0.66 μg/dL, n = 12), a significant 14% reduction in TT4 was observed in *Thrb^{PV/PV}Ncor1^{ΔID/ΔID}* mice (27.91 ± 1.55 μg/dL, n = 12). Therefore, the presence of two mutated alleles of the *Ncor1* gene reduced the elevated serum TT4 in both heterozygous and homozygous *Thrb^{PV}* mice.

Serum TT3 levels were also analyzed from mice of all genotypes (Fig. 2*B*). Compared with WT mice (1.51 ± 0.07 ng/dL, n = 21), a 21% reduction of TT3 was observed in *Thrb^{+/+}Ncor1^{ΔID/ΔID}* mice (1.20 ± 0.06 ng/dL, n = 12). The elevated TT3 concentration in *Thrb^{PV/+}Ncor1^{+/+}* mice (1.92 ± 0. 089 ng/dL, n = 16) decreased by ~15% in *Thrb^{PV/+}Ncor1^{ΔID/ΔID}* mice (1.63 ± 0.08 ng/dL, n = 14). Compared with TT3 in *Thrb^{PV/PV}Ncor1^{+/+}* mice (12.31 ± 1.59 ng/dL, n = 9), a more dramatic 55% reduction was observed in *Thrb^{PV/PV}Ncor1^{ΔID/ΔID}* mice (5.48 ± 0.52 ng/dL, n = 12). Therefore, both the elevated TT4 and TT3 due to the dominant negative action of PV were markedly abrogated by the expression of NCOR1ΔID.

Serum TSH levels were also analyzed, as shown in Fig. 2*C*. No apparent effect was observed in serum TSH levels by the expression of NCOR1ΔID in WT mice (compare data groups 1 and 2) despite the presence of low TH levels. However, the elevated TSH in *Thrb^{PV/+}Ncor1^{+/+}* mice decreased by 35% in *Thrb^{PV/+}Ncor1^{ΔID/ΔID}* mice (compare data groups 3–4) and was similar to that found in WT mice. The highly elevated TSH in *Thrb^{PV/PV}Ncor1^{+/+}* mice was also lowered by the expression of NCOR1ΔID in *Thrb^{PV/PV}Ncor1^{ΔID/ΔID}* mice (30% decrease; compare data groups 5 and 6, Fig. 2*C*). Taken together, these thyroid function tests show that the expression of NCOR1ΔID ameliorates the syndrome of RTH on the pituitary–thyroid axis.
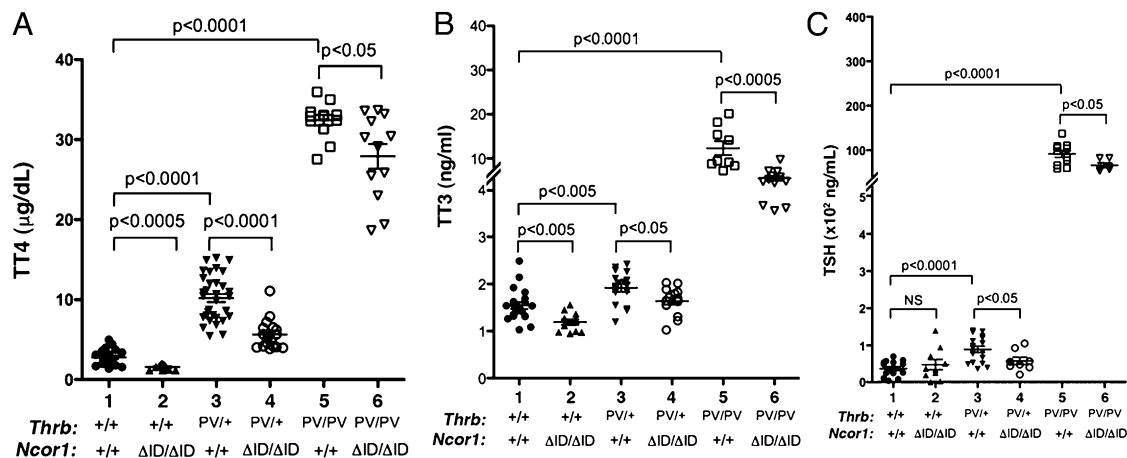

Fig. 2. Thyroid function tests of *Thrb^{PV}* mice with or without mutant NCOR1ΔID. Serum levels of total T4 (*A*), total T3 (*B*), and TSH (*C*) were determined in adult mice (males and females, 3–5 mo old). Each point represents a value for an individual mouse, and the horizontal brackets represent the mean values with the *P* value shown.

MEDICAL SCIENCES

We next examined the effect of the expression of NCOR1ΔID on thyroid growth. No effect of the expression of NCOR1ΔID in $Thrb^{+/+}$ mice on thyroid growth was observed (compare bar 1 to bar 2, Fig. 3A), consistent with previous data (6). Similar to our earlier work (8), the thyroid weights of $Thrb^{PV/+}$ and $Thrb^{PV/PV}$ mice were enlarged ~2- and 23-fold, respectively (Fig. 3A, bar 3 vs. bar 1 and bar 5 vs. bar 1). Although the expression of NCOR1ΔID led to a small decrease in the thyroid weight of $Thrb^{PV/+}$ mice (compare bar 3 to bar 4), a 50% reduction in thyroid weight was clearly evident in $Thrb^{PV/PV}Ncor1^{ΔID/ΔID}$ mice (compare bar 5 to bar 6). Representative examples of thyroids from $Thrb^{PV/PV}Ncor1^{+/+}$ mice and $Thrb^{PV/PV}Ncor1^{ΔID/ΔID}$ mice are shown in Fig. 3B, *Left* and *Right*, respectively. The thyroid of the $Thrb^{PV/PV}Ncor1^{+/+}$ mice was large with the appearance of hypervascularity, whereas that of the $Thrb^{PV/PV}Ncor1^{ΔID/ΔID}$ mice was smaller with a more normal appearance. Consistently, histological analysis showed that the extensive hyperplasia exhibited in the thyroid of $Thrb^{PV/PV}$ mice (Fig. 3Cc) reverted to early hyperplasia (Fig. 3Cc), indicating that proliferation of thyrocytes was inhibited by the expression of NCOR1ΔID in $Thrb^{PV/PV}Ncor1^{ΔID/ΔID}$ mice. In contrast to the thyroid, comparison of the size of pituitaries among mice with different genotypes did not reveal any effects of NCOR1ΔID.

Effect of the Expression of NCOR1ΔID on the RTH Is Target Tissue-Dependent.
Because RTH affects many peripheral target tissues, we also evaluated how the resistance of target tissues was affected by the expression of NCOR1ΔID.

Retarded growth in $Thrb^{PV}$ mice. Consistent with RTH patients, $Thrb^{PV}$ mice exhibit growth retardation by displaying impaired weight gain (8). We therefore assessed how the expression of NCOR1ΔID affects body weight in $Thrb^{PV}$ mice. Fig. 4A shows that, at the age of 4–6 mo, no effect of NCOR1ΔID was apparent in $Thrb^{+/+}$ mice (30.19 ± 2.31 g, $n = 8$ and 29.59 ± 0.95 g, $n = 31$: compare group 2 and group 1, respectively, in Fig. 4A), although when younger than 12 wk of age NCoR^{ΔID} mice were slightly lighter than WT mice as previously described (6). Simi-

larly, the presence of NCORΔID had no effect on the body weight of $Thrb^{PV/+}$ mice (group 4 vs. group 3). However, consistent with previous findings, $Thrb^{PV/PV}Ncor1^{+/+}$ mice displayed impaired growth with a significant 12% reduction in body weight (26.09 ± 0.70 g, $n = 39$: group 5) compared with that of WT mice (group 1). However, this impairment of growth was ameliorated in $Thrb^{PV/PV}Ncor1^{ΔID/ΔID}$ mice (31.33 ± 2.32 g, $n = 9$: group 6) such that the body weight of $Thrb^{PV/PV}Ncor1^{ΔID/ΔID}$ mice was similar to that of WT mice (group 1, Fig. 4A). Thus, the impaired weight of $Thrb^{PV/PV}Ncor1^{+/+}$ mice is normalized when the NCOR1–PV interaction is disrupted.

Although reduced body weight in $Thrb^{PV}$ mice may be secondary to energy expenditure and body composition, it may also be reflected in delayed bone development (8, 16). As shown in Fig. 4B, compared with the average length of femurs of WT mice (15.7 ± 0.11 mm, $n = 8$), the expression of NCOR1ΔID alone leads to a 7% reduction in the lengths of femurs of $Thrb^{+/+}Ncor1^{ΔID/ΔID}$ mice (14.64 ± 0.13 mm, $n = 8$: compare group 2–1), suggesting that the increased sensitivity to TH affects bone development. Consistent with previous findings, a small reduction in femur lengths (~3%) was detected in $Thrb^{PV/+}Ncor1^{+/+}$ mice (15.3 ± 0.11 mm, $n = 9$) compared with WT mice. No additional reduction in the femur lengths as that seen in WT mice (group 2, Fig. 4B) was apparent when NCOR1ΔID was expressed in $Thrb^{PV/+}Ncor1^{ΔID/ΔID}$ mice (group 4 vs. group 3, Fig. 4B). Compared with WT mice, a marked reduction in the lengths of femurs (~10%) was apparent in $Thrb^{PV/PV}Ncor1^{+/+}$ mice (14.22 ± 0.22 mm, $n = 9$). This reduction was not significantly different in $Thrb^{PV/PV}Ncor1^{ΔID/ΔID}$ mice. These results indicate that, although the expression of NCOR1ΔID impaired the development of long bones, this effect was lost in mice harboring a TRβ mutant; furthermore, NCOR1ΔID had no effect on the action of PV in femurs. Thus, the effect of NCORΔID in preventing loss of body weight is not related to its independent effects on bone development.

Abnormalities in the liver of $Thrb^{PV}$ mice. Previously, we found that the livers of $Thrb^{PV}$ mice are enlarged (17). We therefore compared the liver weight among mice with different genotypes (Fig. 5A). The expression of NCOR1ΔID in $Thrb^{+/+}Ncor1^{ΔID/ΔID}$ mice led to an ~24% increase in liver weight (compare group 2 to group 1). The liver of $Thrb^{PV/+}Ncor1^{+/+}$ mice exhibited a small (~10%) but significant increase compared with that of WT mice (group 3 vs. group 1). Interestingly, an additional increase in the weight of liver was detected in $Thrb^{PV/+}Ncor1^{ΔID/ΔID}$ mice (32% increase compared with WT mice: group 4 vs. group 1; 29% increase compared with $Thrb^{PV/+}Ncor1^{+/+}$ mice: group 4 vs. group 3). Consistent with our previous findings, the liver weight of $Thrb^{PV/PV}Ncor1^{+/+}$ mice was markedly increased (62%) compared with that of WT mice (group 5 vs. group 1). A further increase was detected by the expression of NCOR1ΔID in $Thrb^{PV/PV}Ncor1^{ΔID/ΔID}$ mice (200% increase compared with WT mice; 23% increase compared with that of $Thrb^{PV/PV}Ncor1^{+/+}$ mice). These results indicate that NCOR1ΔID acted synergistically with PV to increase liver weight.

In addition to enhanced liver growth, $Thrb^{PV/PV}$ mice exhibit abnormalities in the regulation of serum cholesterol (18). As shown in Fig. 5B, the expression of NCOR1ΔID in $Thrb^{+/+}Ncor1^{ΔID/ΔID}$ mice elevated the serum cholesterol levels from 139.1 ± 6.8 mg/dL ($n = 23$) to 181.1 ± 9.4 mg/dL ($n = 12$) in WT mice. This increase in serum cholesterol is different from what we have seen previously in $Ncor1ΔID$ mice (6) and may be due to the effect of the different genetic backgrounds. A similar increase was detected in $Thrb^{PV/+}Ncor1^{ΔID/ΔID}$ mice (180.4 ± 11.5 mg/dL, $n = 23$: group 4) compared with $Thrb^{PV/+}Ncor1^{+/+}$ mice (133.7 ± 5.9 mg/dL, $n = 19$: group 3). Consistent with our previous findings (18), serum cholesterol levels were elevated 39% in $Thrb^{PV/PV}Ncor1^{+/+}$ mice (193.3 ± 18 mg/dL, $n = 13$) compared with those in WT mice. The elevated serum cholesterol levels were not changed by the expression of NCOR1ΔID in $Thrb^{PV/PV}Ncor1^{ΔID/ΔID}$ mice (group 6 vs. group 5). Thus, the expression of NCOR1ΔID does not improve the metabolism of serum cholesterol in RTH.
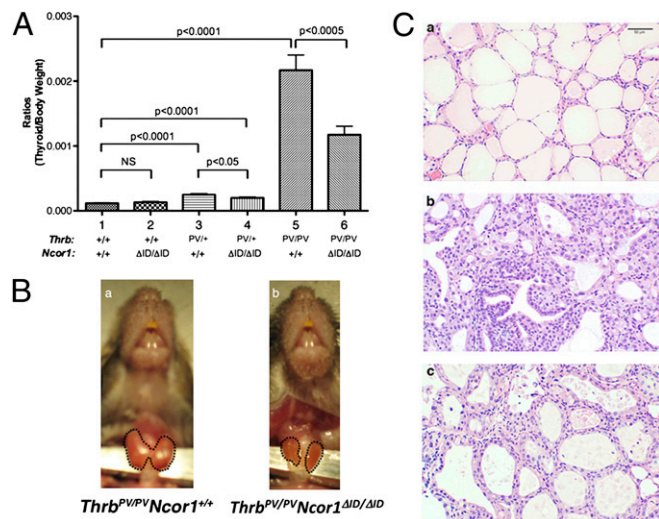

Fig. 3. Comparison of thyroid weight among mice with indicated genotypes. (A) Thyroids were dissected from adult mice (males and females 3–5 mo old). Ratios of tissue mass vs. body weight were determined (thyroid weight/body weight). The data are expressed as mean ± SEM (n = 15–20) with P value indicated. (B) Representative example of a smaller-sized thyroid of a $Thrb^{PV/PV}Ncor1^{ΔID/ΔID}$ mouse compared with the thyroid of a $Thrb^{PV/PV}Ncor1^{+/+}$ mouse. The thyroids in these mice are outlined. (C) Representative histological features of the thyroid gland of $Thrb^{PV}$ mice with or without $Ncor1^{ΔID}$. Hematoxylin and eosin staining of thyroids from 3- to 5-mo-old (a) WT, (b) $Thrb^{PV/PV}Ncor1^{+/+}$, and (c) $Thrb^{PV/PV}Ncor1^{ΔID/ΔID}$ mice. All panels are shown with the same magnification.
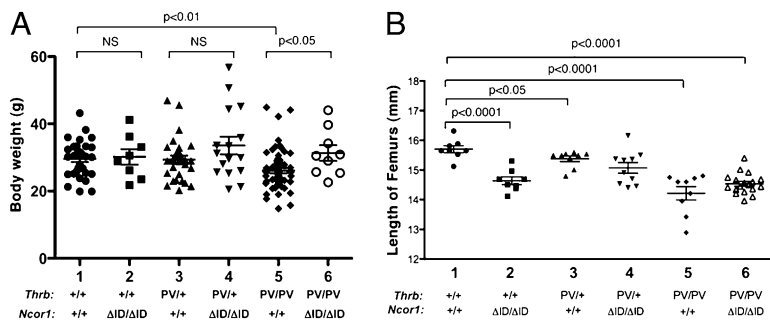
Fig. 4. Effect of NCOR1ΔID on growth. Comparison of body weight (*A*) and length of femurs (*B*) among adult mice (males and females 3–5 mo old) with indicated genotypes. The difference in body weight between $Thrb^{PV/PV} Ncor1^{+/+}$ and $Thrb^{PV/PV} Ncor1^{ΔID/ΔID}$ mice (*A*) is significant ($P < 0.05$), as determined by Student's *t* test analysis. (*B*) Length of femurs did not show any significant difference in $Thrb^{PV/PV} Ncor1^{+/+}$ and $Thrb^{PV/PV} Ncor1^{ΔID/ΔID}$ mice.

Effect of NCOR1ΔID on PV-Mediated Gene Expression Patterns Is Target Gene-Dependent. Our observation that the loss of the PV–NCOR1 interaction led to a decrease in the serum TSH levels of $Thrb^{PV}$ mice (Fig. 2*C*) prompted us to examine whether the reduction of serum TSH is mediated at the level of transcription. We analyzed the expression of the TSHβ subunit gene (*Tshb*) and α-glycoprotein common subunit (*Cga*) genes in the pituitary gland. As shown in Fig. 6*A*a, the elevation of *Tshb* mRNA expression found in $Thrb^{PV/+} Ncor1^{+/+}$ mice (bar 3) is reversed to the level of WT mice (bar 1) in $Thrb^{PV/+} Ncor1^{ΔID/ΔID}$ mice (bar 4). The highly elevated *Tshb* mRNA in $Thrb^{PV/PV} Ncor1^{+/+}$ mice (bar 5) was reduced 70% in $Thrb^{PVPV} Ncor1^{ΔID/ΔID}$ mice (bar 6). Thus, the elevation of *Tshb* mRNA by PV is prevented when the PV–NCOR1 interaction is blocked. We also examined whether the expression of the *Cga* gene was affected by NCOR1ΔID (Fig. 6*A*b). In $Ncor1^{ΔID}$ mice, the expression of the *Cga* gene moderately decreased (20%) compared with WT mice (bar 2 vs. bar 1: Fig. 6*A*b), but the elevated *Cga* mRNA due to the dominant negative effect of PV in $Thrb^{PV/PV} Ncor1^{+/+}$ mice (bar 5) was not affected in $Thrb^{PVPV} Ncor1^{ΔID/ΔID}$ mice (compare bar 6 to bar 5: Fig. 6*A*, *b*). Thus, these data suggest that the activation of the *Cga* expression by PV does not require NCOR1.

In addition to the above negatively regulated genes, we also examined T3-postively regulated genes in the liver of $Thrb^{PV}$ mice (Fig. 6*B*). The malic enzyme gene (*Me1*) is a direct T3-regulated gene. Compared with expression in WT mice, a 2.4-fold increase in the expression of the *Me1* gene was found in $Thrb^{+/+} Ncor1^{ΔID/ΔID}$ mice (bar 2 vs. bar 1). A change in *Me1* gene expression in $Thrb^{PV/+}$ mice similar to that in WT mice was detected in $Thrb^{PV/+} Ncor1^{ΔID/ΔID}$ mice (bars 3 and 4). In $Thrb^{PV/PV} Ncor1^{+/+}$ mice, the expression of the *Me1* gene decreased by 60% (bar 5). This PV-mediated repressed expression in $Thrb^{PV/PV} Ncor1^{+/+}$ mice was blocked by the expression of NCOR1ΔID in $Thrb^{PV/PV} Ncor1^{ΔID/ΔID}$ mice and reverted to a level that was threefold higher than that in WT mice (compare bar 6 to bar 1). We next examined the expression of cholesterol 7a hydroxylase 1 (*Cyp7a1*), the rate-limiting enzyme that mediates the conversion of cholesterol into bile acids and a known T3 target gene; its dysregulation has been shown to potentially mediate the hypercholesterolemia seen in

RTH (Fig. 6*B*b). Similar to *Me1*, the expression of the *Cyp7a1* mRNA was increased 2.8-fold in $Thrb^{+/+} Ncor1^{ΔID/ΔID}$ mice vs. WT mice. In contrast, PV alone mediated 40 and 60% repression in the expression of the *Cyp7a1* mRNA in $Thrb^{PV/+} Ncor1^{+/+}$ mice and in $Thrb^{PV/PV} Ncor1^{+/+}$ mice, respectively (bars 3 and 5: Fig. 6*B*b). However, the PV-mediated repression was blocked by the expression of NCOR1ΔID in $Thrb^{PV/+} Ncor1^{ΔID/ΔID}$ mice and reverted to 1.5-fold (bar 4) higher than that in WT mice (bar 1). In $Thrb^{PV/PV} Ncor1^{ΔID/ΔID}$ mice, the PV-mediated repression was also blocked (bar 6). However, the degree of reversal of the PV-mediated repression was smaller than that in $Thrb^{PV/+} Ncor1^{ΔID/ΔID}$ mice (compare bar 6 to bar 4).

We further evaluated the effect of NCOR1ΔID on the expression of the CCAAT/enhancer-binding protein α (*C/ebpα*) gene, a known T3-target gene in the liver. Fig. 6*B*c, shows that the expression of the *C/ebpα* gene was repressed by ~50% in $Thrb^{+/+}$ mice by the expression of NCOR1ΔID (bar 2 vs. bar 1). Compared with WT mice, a small but significant decrease (~15%) in the expression of the *C/ebpα* gene was detected in $Thrb^{PV/+} Ncor1^{+/+}$ mice and in $Thrb^{PV/PV} Ncor1^{+/+}$ mice (compare bars 3 and 5 to bar 1), which was further repressed by NCOR1ΔID (bars 4 and 6). Thus, in contrast to the expression patterns of the *Me1* and *Cyp7a1* genes, the PV-mediated repression of the *C/ebpα* gene was intensified by NCOR1ΔID (bar 6 vs. bar 5). Thus, the effect of NCOR1ΔID on the PV-mediated abnormal expression of positively regulated genes in the liver is target gene dependent.

Discussion

Although it is an uncommon clinical entity, RTH has long been a model by which to understand thyroid hormone action both clinically and at the molecular level. In addition, RTH has been a model used to understand how mutations in other nuclear receptors mediate disease. The nature of the mutations found in RTH and their effect on the structure of the TRβ isoform have suggested that the disease could be mediated by a defect in the release or recruitment of coregulatory proteins to TRβ rather than simply by the inability of the TRβ to bind ligand. This idea is supported by the fact that deletion of one TRβ allele causes no
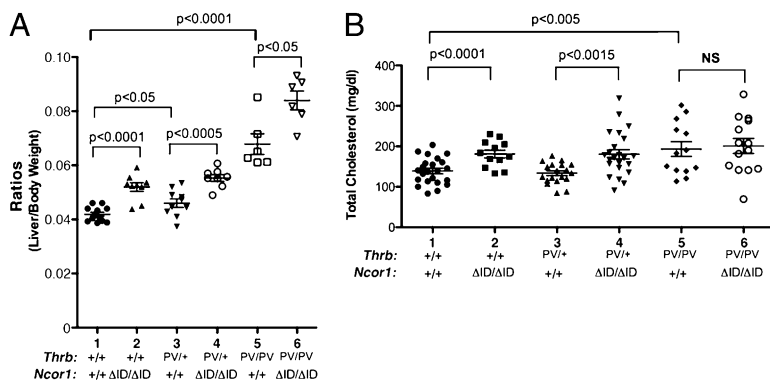

Fig. 5. The liver of mice expressing NCOR1ΔID is enlarged. (*A*) The livers from adult mice (males 3–5 mo old) for each genotype were dissected out and compared. Ratios of tissue mass vs. body weight were determined (liver weight:body weight). (*B*) Serum total cholesterol levels were determined from adult mice (males and females 3–5 mo old), as described in *Materials and Methods*. Data are expressed as mean values ± SEM ($n = 15$–20) with *P* values shown.
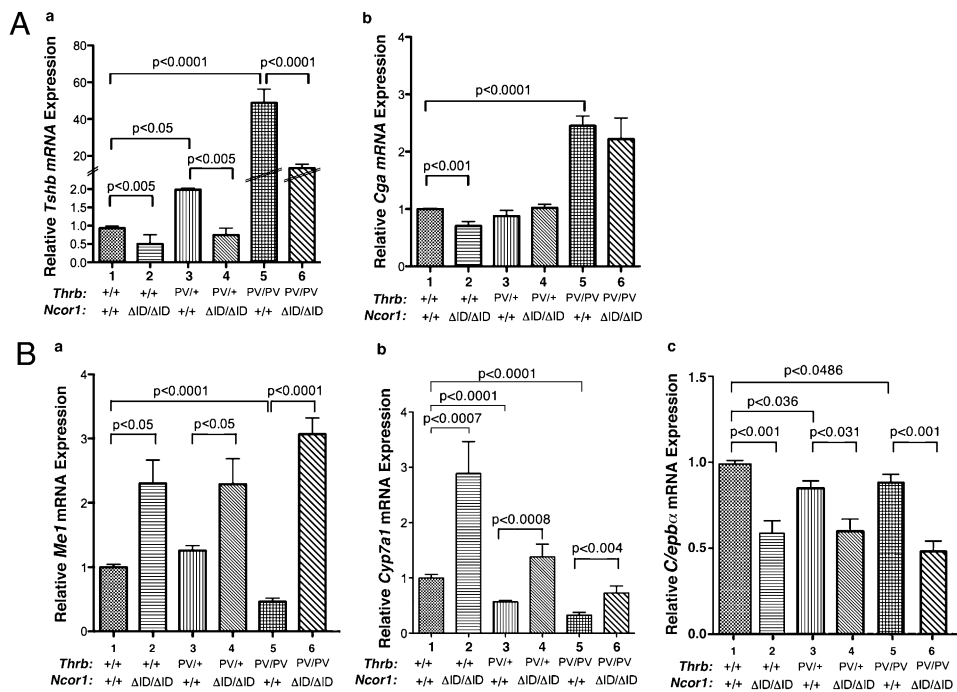
Fig. 6. Effect of NCOR1ΔID on PV-mediated gene expression patterns is T3-target gene-dependent. (*A*) Comparison of the expression of the TSH β-subunit gene (*Tshb*) and α-glycoprotein common subunit (*Cga*) in the pituitary of *Thrb^PV* mice with or without NCOR1ΔID. (*B*) Comparison of the expression of malic enzyme (*Me1*), cholesterol 7α hydroxylase1 (*Cyp7a1*), and CCAAT/enhancer-binding protein α (*C/ebpα*) mRNA in the liver of *Thrb^PV* mice. Relative quantification of each target mRNA was determined by arbitrarily setting the control value of WT mice as 1. The level of expression was normalized by signals obtained using specific primers for mouse *Gadph*. The data are expressed as mean values ± SEM (n = 6–9) with P values shown.

disease whereas the expression of a single-mutant TRβ allele leads to RTH because of its dominant negative properties (7, 19). Thus, understanding the molecular pathogenesis of RTH could have significant ramifications for both its treatment and the treatment of other nuclear receptor resistance syndromes in humans.

To address the molecular pathogenesis of RTH in vivo, we introduced a mutant *Ncor1* allele (*Ncor1^ΔID*) into a mouse model of RTH (the *Thrb^PV* mouse) that faithfully recapitulates this human disease (8), with evidence of both central and peripheral resistance to TH in the presence of one mutant allele and severe resistance in the homozygous state. Importantly, the fact that NCOR1ΔID cannot interact with either the TRβ (5, 6) or PV in vivo (Fig. 1*B*) has allowed us to test directly whether NCOR1 mediates the detrimental effects of PV. Remarkably, the elevations in TSH, TT4, and TT3 found in either *Thrb^PV/+* or *Thrb^PV/PV* mice are modestly but significantly reversed in the presence of two *Ncor1^ΔID* alleles. The fact that the effects are greater in *Thrb^PV/+* mice than in *Thrb^PV/PV* mice suggests that the homozygous state might allow for the recruitment of additional corepressors such as NCOR2. This result also establishes the role of a mutated TRβ, PV, and NCOR1 in mediating the central resistance seen in RTH as the introduction of NCOR1ΔID also prevents the elevation in *Tshb* gene expression seen in either *Thrb^PV/+* mice or *Thrb^PV/PV* mice (Fig. 6*A*a). Given that the defects in the central regulation of the thyroid axis are necessary for the development and diagnosis of RTH, their partial correction in the presence of NCOR1ΔID suggests that therapies targeting the TR–NCOR1 complex could be therapeutic in RTH.

Although the introduction of NCORΔID into *Thrb^PV/PV* mice lowered serum TSH by 35%, it appeared to have a far more dramatic effect on the thyroid size, pathological hyperplasia, and vascularity seen in the thyroids from *Thrb^PV/PV* mice. Indeed, this effect is consistent with the proliferative effect of PV and its potential role in the development of thyroid carcinoma being dependent upon NCOR1 recruitment in the follicular cell (20, 21). This cell-autonomous role of NCOR1 in the follicular cell is supported by the decreased ability of *Thrb^+/+Ncor1^ΔID/ΔID* mice to release T4 and T3 in response to TSH, suggesting that NCOR1 controls thyroid hormone action within the follicular cell. Further studies will be required to demonstrate the effect of the PV–NCOR1 interaction on thyroid growth.

In addition to correcting central resistance to RTH in *Thrb^PV/+* mice or *Thrb^PV/PV* mice, the introduction of *Ncor1ΔID* to *Thrb^PV* mice also improved peripheral markers of hormone resistance. The lower body weight seen in *Thrb^PV/PV* mice, potentially a marker of increased energy expenditure in RTH, is increased in the presence of the mutated allele *Ncor1ΔID* (22). This result could be partly due to an increase in liver weight. This possibility is supported by regression analysis that shows a highly significant correlation (R^2 = 0.807, P < 0.001) between liver weight and body weight across the two genotypes (*Thrb^PV/PVNcor1^+/+* and *Thrb^PV/PVNcor1^ΔID/ΔID* mice), suggesting that the liver weight had an impact on the increased body weight of *Thrb^PV/PVNcor1^ΔID/ΔID* mice. In contrast, despite lower TH levels in *Thrb^PV/+* or *Thrb^PV/PV* mice expressing NCOR1ΔID, expression of TH target genes (*Me1* and *Cyp7a1*) in the liver is enhanced, an outcome consistent with inhibition of the dominant effect of the TRβ mutant (23). However, this effect is not present in all genes, as indicated by the findings that the repression of the *C/ebpα* gene is not reversed in mice expressing NCOR1ΔID, again indicating that the mutant TR can potentially recruit other corepressors. Furthermore, the elevated cholesterol levels found in *Thrb^PV/PV* mice, which are secondary to repression of the *Cyp7a1* gene, are not reversed in *Thrb^PV/PV* mice expressing NCOR1ΔID despite enhanced expression of the *Cyp7a1* gene. The sustained elevated cholesterol level is likely due to the primary effect of NCOR1ΔID on enhancing cholesterol synthesis that we have shown previously and may also explain the increase in liver weight seen in mice that express NCOR1ΔID (5).

Surprisingly, despite the correction of TH levels in *Thrb^PV/+* and *Thrb^PV/PV* mice expressing NCOR1ΔID, the hyperthyroid bone phenotype present in *Thrb^PV/+* and *Thrb^PV/PV* mice was not corrected. Indeed, it is well established that the bone phenotype present in *Thrb^PV/+* and *Thrb^PV/PV* mice is the result of juvenile hyperthyroidism with increased ossification and postnatal shortening of bone length due to the excessive actions of the high circulating levels of TH working through the wild-type TRα1 present in bone (8, 24). Thus, falling TH levels in *Thrb^PV/+* and *Thrb^PV/PV* mice expressing NCOR1ΔID would be expected to correct this defect, similar to what was seen with body weight. However, it also clear that *Ncor1^ΔID* mice independently have increased sensitivity to TH and in fact also have a shortened femur length that approaches that found in *Thrb^PV* mice. Thus, it is likely that this premature fusion of the growth plate in

$Ncor1^{\Delta ID}$ mice occurring in the setting of low TH levels could prevent the reversal mediated by the expressed NCOR1ΔID in $Thrb^{PV/+}$ and $Thrb^{PV/PV}$ mice.

In summary, in this study we have established that a mutant TRβ that causes RTH mediates many of its effects by the aberrant recruitment of NCOR1. By preventing the recruitment of NCOR1 in vivo, the RTH phenotype is alleviated centrally and in some peripheral tissues. However, because NCOR1 also mediates sensitivity to TH in the context of TRα1 signaling in bone, the hyperthyroid phenotype in that tissue cannot be reversed. Nonetheless, in view of the lack of effective treatment for RTH so far, the present results suggest that novel therapeutic strategies that target the TR–NCOR1 interaction may benefit patients with RTH.

Materials and Methods

Mouse Strains. This animal study was carried out according to the protocol approved by the National Cancer Institute Animal Care and Use Committee. Mice harboring the $Thrb^{PV}$ gene ($Thrb^{PV}$ mice) were prepared and genotyped as described earlier (8). $Ncor1^{\Delta ID}$ mice were prepared as described by Astapova et al. (6). $Thrb^{PV/PV}Ncor1^{\Delta ID/\Delta ID}$ mice were bred by crossing $Thrb^{+/+}$ $Ncor1^{\Delta ID/ID}$ mice with $Thrb^{PV/+}$ mice, followed by crossing $Thrb^{PV/+}Ncor1^{\Delta ID/\Delta ID}$ mice with $Thrb^{PV/+}Ncor1^{\Delta ID/\Delta ID}$ mice. Mice with different genotypes used in the present study were intercrossed several generations, and littermates with a similar genetic background were used in all experiments.

Hormone Assays. The serum levels of total T4 and total T3 were determined using a Gamma Coat T4 and T3 assay RIA kit (DiaSorin). Serum TSH levels were measured as previously described (25). A cholesterol E kit (Stanbio Laboratory) was used for quantitative determination of total cholesterol in mouse serum.

RNA Isolation and Quantitative Real-Time RT-PCR. Total RNA was extracted from pituitary and liver of mice using TRIzol (Invitrogen). Quantitative real-time RT-PCR was performed with a Quantitect SYBR Green RT-PCR kit (QIAGEN), according to the manufacturer's instructions and using a Light-Cycler thermal cycler (Roche Diagnostics). Total RNA (200 ng) was used in RT-PCR determinations as described previously (26). The specific primer sequences are available upon request.

Coimmunoprecipitation. 293T cells were plated at a density of 1×10^6 in a 10-cm dish and transfected with 4 μg of expression plasmid for $Ncor1$ or $Ncor1\Delta ID$ using Lipofectamine 2000. At the same time, cells were infected with adenoviruses encoding Flag-tagged PV at a multiplicity of infection (MOI) of 10. After lysing the cells, immunoprecipitation (1 mg of total lysates) was carried out using monoclonal anti-PV antibody (#302; 4 μg) or IgG as negative control followed by Western blot analysis using polyclonal affinity-purified anti-NCOR1 antibodies [PHQQ; generated against a C-terminal NCoR peptide (PHQQNRIWEREPAPLLSAQ); 2 μg/mL].

In vivo coimmunoprecipitaton was carried out using nuclear extracts prepared from livers of $Thrb^{PV/PV}Ncor1^{+/+}$ mice and $Thrb^{PV/PV}Ncor1^{\Delta ID/\Delta ID}$ mice, as described previously (27). Nuclear extracts (1.1 mg protein) were incubated overnight with 5 μg of a mouse monoclonal anti-TR (C4), anti PV (#302), or anti-MOPC (Sigma Inc, MOPC141). MOPC contains IgG2b, k derived from ascites originated from mineral oil-induced plasmacytoma. Bound proteins were analyzed by SDS/PAGE followed by Western blot analysis using PHQQ.

Histological Analysis. The thyroid gland was dissected and embedded in paraffin. Five-micrometer-thick sections were prepared and stained with hematoxylin and eosin. For each animal, single random sections through the thyroid were examined.

Statistical Analysis. All data are expressed as mean ± the SEM. Differences between groups were examined for statistical significance using Student's t test with the use of GraphPad Prism 4.0a (GraphPad Software). $P < 0.05$ is considered statistically significant.

1. Hollenberg AN, Forrest D (2008) The thyroid and metabolism: The action continues. *Cell Metab* 8:10–12.
2. Cheng SY (2000) Multiple mechanisms for regulation of the transcriptional activity of thyroid hormone receptors. *Rev Endocr Metab Disord* 1:9–18.
3. Glass CK, Rosenfeld MG (2000) The coregulator exchange in transcriptional functions of nuclear receptors. *Genes Dev* 14:121–141.
4. Alenghat T, et al. (2008) Nuclear receptor corepressor and histone deacetylase 3 govern circadian metabolic physiology. *Nature* 456:997–1000.
5. Astapova I, et al. (2008) The nuclear corepressor, NCoR, regulates thyroid hormone action in vivo. *Proc Natl Acad Sci USA* 105:19544–19549.
6. Astapova I, et al. (2011) The nuclear receptor corepressor (NCoR) controls thyroid hormone sensitivity and the set point of the hypothalamic-pituitary-thyroid axis. *Mol Endocrinol* 25:212–224.
7. Refetoff S, Weiss RE, Usala SJ (1993) The syndromes of resistance to thyroid hormone. *Endocr Rev* 14:348–399.
8. Kaneshige M, et al. (2000) Mice with a targeted mutation in the thyroid hormone beta receptor gene exhibit impaired growth and resistance to thyroid hormone. *Proc Natl Acad Sci USA* 97:13209–13214.
9. Hashimoto K, et al. (2001) An unliganded thyroid hormone receptor causes severe neurological dysfunction. *Proc Natl Acad Sci USA* 98:3998–4003.
10. Cheng SY (2004) New development in thyroid hormone resistance. *Hot Thyroidology* January, No. 1.
11. Yen PM, Sugawara A, Refetoff S, Chin WW (1992) New insights on the mechanism(s) of the dominant negative effect of mutant thyroid hormone receptor in generalized resistance to thyroid hormone. *J Clin Invest* 90:1825–1831.
12. Liu Y, Takeshita A, Misiti S, Chin WW, Yen PM (1998) Lack of coactivator interaction can be a mechanism for dominant negative activity by mutant thyroid hormone receptors. *Endocrinology* 139:4197–4204.
13. Safer JD, Cohen RN, Hollenberg AN, Wondisford FE (1998) Defective release of corepressor by hinge mutants of the thyroid hormone receptor found in patients with resistance to thyroid hormone. *J Biol Chem* 273:30175–30182.
14. Agostini M, et al. (2006) Non-DNA binding, dominant-negative, human PPARgamma mutations cause lipodystrophic insulin resistance. *Cell Metab* 4:303–311.
15. Parrilla R, Mixson AJ, McPherson JA, McClaskey JH, Weintraub BD (1991) Characterization of seven novel mutations of the c-erbA beta gene in unrelated kindreds with generalized thyroid hormone resistance. Evidence for two "hot spot" regions of the ligand binding domain. *J Clin Invest* 88:2123–2130.
16. O'Shea PJ, et al. (2003) A thyrotoxic skeletal phenotype of advanced bone formation in mice with resistance to thyroid hormone. *Mol Endocrinol* 17:1410–1424.
17. Araki O, Ying H, Zhu XG, Willingham MC, Cheng SY (2009) Distinct dysregulation of lipid metabolism by unliganded thyroid hormone receptor isoforms. *Mol Endocrinol* 23:308–315.
18. Kamiya Y, et al. (2003) Modulation by steroid receptor coactivator-1 of target-tissue responsiveness in resistance to thyroid hormone. *Endocrinology* 144:4144–4153.
19. Forrest D, Vennström B (2000) Functions of thyroid hormone receptors in mice. *Thyroid* 10:41–52.
20. Suzuki H, Willingham MC, Cheng SY (2002) Mice with a mutation in the thyroid hormone receptor beta gene spontaneously develop thyroid carcinoma: A mouse model of thyroid carcinogenesis. *Thyroid* 12:963–969.
21. Guigon CJ, Cheng SY (2009) Novel oncogenic actions of TRbeta mutants in tumorigenesis. *IUBMB Life* 61:528–536.
22. Mitchell CS, et al. (2010) Resistance to thyroid hormone is associated with raised energy expenditure, muscle mitochondrial uncoupling, and hyperphagia. *J Clin Invest* 120:1345–1354.
23. Gullberg H, Rudling M, Forrest D, Angelin B, Vennström B (2000) Thyroid hormone receptor beta-deficient mice show complete loss of the normal cholesterol 7alpha-hydroxylase (CYP7A) response to thyroid hormone but display enhanced resistance to dietary cholesterol. *Mol Endocrinol* 14:1739–1749.
24. O'Shea PJ, Bassett JH, Cheng SY, Williams GR (2006) Characterization of skeletal phenotypes of TRalpha1 and TRbeta mutant mice: Implications for tissue thyroid status and T3 target gene expression. *Nucl Recept Signal* 4 e011.
25. Furumoto H, et al. (2005) An unliganded thyroid hormone beta receptor activates the cyclin D1/cyclin-dependent kinase/retinoblastoma/E2F pathway and induces pituitary tumorigenesis. *Mol Cell Biol* 25:124–135.
26. Ying H, et al. (2003) Alterations in genomic profiles during tumor progression in a mouse model of follicular thyroid carcinoma. *Carcinogenesis* 24:1467–1479.
27. Zhang XY, et al. (2002) Differential expression of thyroid hormone receptor isoforms dictates the dominant negative activity of mutant Beta receptor. *Mol Endocrinol* 16:2077–2092.

MEDICAL SCIENCES